Optical properties of anatase and rutile TiO_2 studied by GGA+U*

Jinping Li(李金平)[1,3,†], Songhe Meng(孟松鹤)[1], Liyuan Qin(秦丽媛)[1], and Hantao Lu(陆汉涛)[2]

[1] *Center for Composite Materials and Structures, Harbin Institute of Technology, Harbin* 150080, *China*
[2] *Center for Interdisciplinary Studies & Key Laboratory for Magnetism and Magnetic Materials (Ministry of Education), Lanzhou University, Lanzhou* 730000, *China*
[3] *Yukawa Institute for Theoretical Physics, Kyoto University, Kyoto* 606-8502, *Japan*

(Received 1 November 2016; revised manuscript received 2 May 2017; published online 20 June 2017)

The optical properties of thermally annealed TiO_2 samples depend on their preparation process, and the TiO_2 thin films usually exist in the form of anatase or rutile or a mixture of the two phases. The electronic structures and optical properties of anatase and rutile TiO_2 are calculated by means of a first-principles generalized gradient approximation (GGA) +U approach. By introducing the Coulomb interactions on 3d orbitals of Ti atom (U^{d}) and 2p orbitals of O atom (U^{p}), we can reproduce the experimental values of the band gap. The optical properties of anatase and rutile TiO_2 are obtained by means of the GGA+U method, and the results are in good agreement with experiments and other theoretical data. Further, we present the comparison of the electronic structure, birefringence, and anisotropy between the two phases of TiO_2. Finally, the adaptability of the GGA+U approach has been discussed.

Keywords: TiO_2, first-principles, GGA+U, electronic structure, optical properties

PACS: 71.15.–m, 71.15.Mb, 78.20.Ci, 78.20.Fm **DOI:** 10.1088/1674-1056/26/8/087101

1. Introduction

TiO_2, as one of the wide band-gap semiconductors, with stable, nontoxic, and efficient photocatalytic activity, has been widely used in photocatalytic, solar battery, sensor, self-cleaning materials, and so on.[1–4] TiO_2 thin films usually exist in two polymorphs after high-temperature annealing, i.e., the anatase and the rutile, shorted as a-TiO_2 and r-TiO_2, respectively.[5–9]

In experiments, optical properties of thermally annealed TiO_2 have shown intrinsic birefringence and anisortropy in some samples.[10] For example, the fundamental optical properties of optically anisotropic materials such as r-TiO_2 have been measured at room temperature with linearly polarized light of wavelength longer than 110 nm.[7] Polarized reflection spectra of single-crystal a-TiO_2 have been obtained in a photon energy range from 2 eV to 25 eV by using synchrotron orbital radiations, and the optical properties show anisotropy.[8] Spectroscopic ellipsometry measurements were made on thin-film and single-crystal a-TiO_2 using a two-modulator generalized ellipsometer. The results show that the complex refractive indices and dielectric function in a- and r-TiO_2 are quite different. Below the band edge, compared with a-TiO_2, r-TiO_2 has a higher refractive index, as well as greater value of birefringence.[9]

Theoretically, the crystal structure, the band structure, and the density of states of a-TiO_2 have been analyzed by using a first-principles local density approximation (LDA) approach.[11] The resulting band-gap value is 2.25 eV. Near the absorption edge, it shows a significant optical anisotropy between the components with directions parallel and perpendicular to the c axis.

In the case of r-TiO_2, the structure and electronic properties have been calculated by using "soft-core" *ab-initio* pseudopotentials constructed within the local density approximation (LDA), and the resulting band-gap value is 2.0 eV. The obtained dielectric function and reflectivity of r-TiO_2 for polarization vector also display difference between the directions parallel and perpendicular to the c axis.[12]

The self-consistent orthogonalized linear-combination-of-atomic-orbitals method in LDA has been used to study the electronic structure and optical properties of the three phases of TiO_2.[13] The obtained band-gap values of a-TiO_2 and r-TiO_2 are 2.04 eV and 1.78 eV, smaller than the experimental data, 3.2 eV and 3.0 eV, respectively. The theoretical calculations show a little difference in the optical properties of the three phases in TiO_2.

Regardless of the above computational efforts, the physical mechanism for the intrinsic birefringence and anisotropy of the optical properties of TiO_2 found in some samples remains to be understood. Note that the band gaps obtained by the previous methods are significantly lower than the experimental values. So, it is important to investigate the electronic structures of a-TiO_2/r-TiO_2 and clarify the difference of optical properties based on the first-principles band structure calculations with electronic correlations to be taken into account

*Project supported by the National Natural Science Foundation of China (Grant Nos. 11672087, 11272107, and 11402252).
†Corresponding author. E-mail: lijinping@hit.edu.cn
© 2017 Chinese Physical Society and IOP Publishing Ltd

effectively.

The LDA+U method has been employed to investigate the properties of r-TiO_2. The results are dramatically improved when additional correlation corrections are introduced on the O 2p orbitals in the LDA+$U^d + U^p$ approach.[14] The experimental band-gap value (3.20 eV) can be reproduced when $U^d = 8.0$ eV and $U^p = 7.0$ eV. In a similar approach, the influence of oxygen defects upon the electronic properties of Nb-doped TiO_2 was studied, and the effective U parameter $U_{eff} = 7.2$ eV has been used to correct the strong Coulomb interaction between 3d electrons localized on Ti in anatase models.[15] The calculated results show that the anatase NbTi cells are degenerated semiconductors with a typical n-type degenerated characteristic in their electronic structure, which is in good agreement with the experimental evidence that anatase Nb:TiO_2 film is an intrinsic transparentmetal. Other researchers set up a model for $Zn_{1-x}Ag_xO$ ($x = 0$, 0.0278, 0.0417) to calculate the geometric structure and energy via the method of generalized gradient approximation (GGA+U), showing that the absorption spectrum in these systems all coincide with experimental data.[16]

In this paper, we use the GGA+U scheme formulated by Loschen *et al.*,[17] to calculate the electric structures and optical properties of r-TiO_2 and a-TiO_2. The on-site Coulomb interactions of 3d orbitals on Ti atom (U^d) and of 2p orbitals on O atom (U^p) are determined so as to reproduce the experimental value of the band gap for the two phases of TiO_2. The comparison of the electronic structure, birefringence and anisotropy between the two phases of TiO_2 is also presented. Finally, the adaptability of the GGA+U approach has been discussed.

2. Computational methodology

Density functional theory (DFT) calculations are performed with plane-wave ultrasoft pseudopotential, by using the GGA with the Perdew–Burke–Ernzerhof (PBE) functional and the GGA+U approach as implemented in the CASTEP code (Cambridge Sequential Total Energy Package).[18] The ionic cores are represented by ultrasoft pseudopotentials for Ti and O atoms. For the Ti atom, the configuration is [Ar] $3d^2 4s^2$, where the $3s^2$, $3p^6$, $3d^2$, and $4s^2$ electrons are explicitly treated as valence electrons. For the O atom, the configuration is [He] $2s^2 2p^4$, where $2s^2$ and $2p^4$ electrons are explicitly treated as valence electrons. The plane-wave cut off energy is 380 eV and the Brillouin-zone integration is performed over the 24×24×24 grid sizes using the Monkorst–Pack method for geometry structure optimization. This set of parameters assures the total energy convergence of 5.0×10^{-6} eV/atom, the maximum force of 0.01 eV/Å, the maximum stress of 0.02 GPa and the maximum displacement of 5.0×10^{-4} Å. We calculated the electronic structures and the optical properties of a-TiO_2 and r-TiO_2 by means of the GGA method without U and GGA+$U^d + U^p$ after having optimized the geometry structure. The details of the calculation have been shown elsewhere.[19]

3. Results and discussion

The space group of a-TiO_2 is $I4_1/amd$ and the local symmetry is C4h-19, and r-TiO_2 is $P4_2/mnm$ and $D4h$-14. The lattice constants a and c are experimentally determined to be $a = 0.3785$ nm and $c = 0.9515$ nm, $a = 0.4593$ nm and $c = 0.2959$ nm,[20,21] respectively. The GGA calculation of the perfect bulk a-TiO_2 and r-TiO_2 is performed to determine the optimized parameters in order to check the applicability and accuracy of the ultrasoft pseudopotential. The optimized parameters are $a = 0.3795$ nm and $c = 0.9837$ nm, and $a = 0.4645$ nm, and $c = 0.2968$ nm for a-TiO_2 and r-TiO_2, respectively, in good agreement with experimental and other theoretical values.[10–13] However, the value of the band gap E_g in a-TiO_2 and r-TiO_2 is around 2.16 eV and 1.85 eV, respectively, smaller than the experimental value of 3.23 eV[22] and 3.0 eV.[23] This is due to the fact that the DFT results often undervalue the energy of 3d orbitals of the Ti atom, lowering the bottom level of conduction bands. As a result, E_g of TiO_2 obtained by GGA is lower than the experimental one.

In order to reproduce the band gap, we first introduce U^d for 3d orbitals of the Ti atom. Using the experimental lattice parameters, we optimize the geometry structure and calculate the band structure and density of state (DOS) of r-TiO_2. The band gap E_g obtained from the band structure is shown in Fig. 1(a) as a function of U^d. It can be seen that E_g firstly increases, and then drops with increasing U^d, showing a maximum value (2.46 eV) at $U^d = 6.75$ eV, where the lattice parameters of the optimized structure are $a = 0.4664$ nm and $c = 0.3086$ nm. The maximum value is smaller than the experimental one (3.0 eV). The saturation of E_g with U^d may be related to the approach of 3d states toward 4s and 3p states, though the microscopic mechanism is not yet fully understood. Next, we introduce U^p for 2p orbital of O atom, while keeping $U^d = 6.75$ eV. The results in Fig. 1(b) show that E_g monotonically increases with U^p. When $U^d = 6.75$ eV and $U^p = 3.5$ eV, the calculated band gap of r-TiO_2 is 3.0 eV, well consistent with the experiment one, where the lattice parameters of the optimized structure are $a = 0.4664$ nm and $c = 0.3082$ nm. For a-TiO_2, when $U^d = 7.75$ eV and $U^p = 1.0$ eV, the calculated band gap of a-TiO_2 is 3.229 eV, well coinciding with the experiment one, where the lattice parameters of the optimized structure are $a = 0.38891$ nm and $c = 0.9870$ nm.

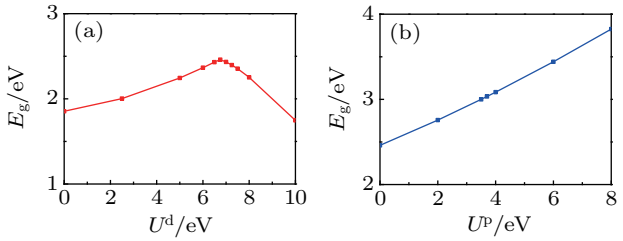


Fig. 1. (color online) Calculated band gap E_g of r-TiO_2 as a function of (a) U^d and (b) U^p.

By adopting these U values: $U^d = 6.75$ eV and $U^p = 3.5$ eV, ($U^d = 7.75$ eV and $U^p = 1.0$ eV for a-TiO_2), we perform the GGA+U calculation for r-TiO_2. The band dispersion is shown in Fig. 2(a). The bottom of the conduction band is located at the G/B point. Since the bottom shifts to higher energy with U^d accompanied by the reconstruction of the conduction band, the separated density of states at 3.03 eV and 6.26 eV obtained by the generalized gradient approximation without U (not shown here) merges to one sharp structure at 3.74 eV as shown in Fig. 2(b). The conduction band is predominantly constructed by Ti 3d states, while the valence band is by O 2p states (as shown in Fig. 2(c) and Fig. 2(d)). Therefore, the excitations across the gap are mainly from the O 2p states to the Ti 3d states.

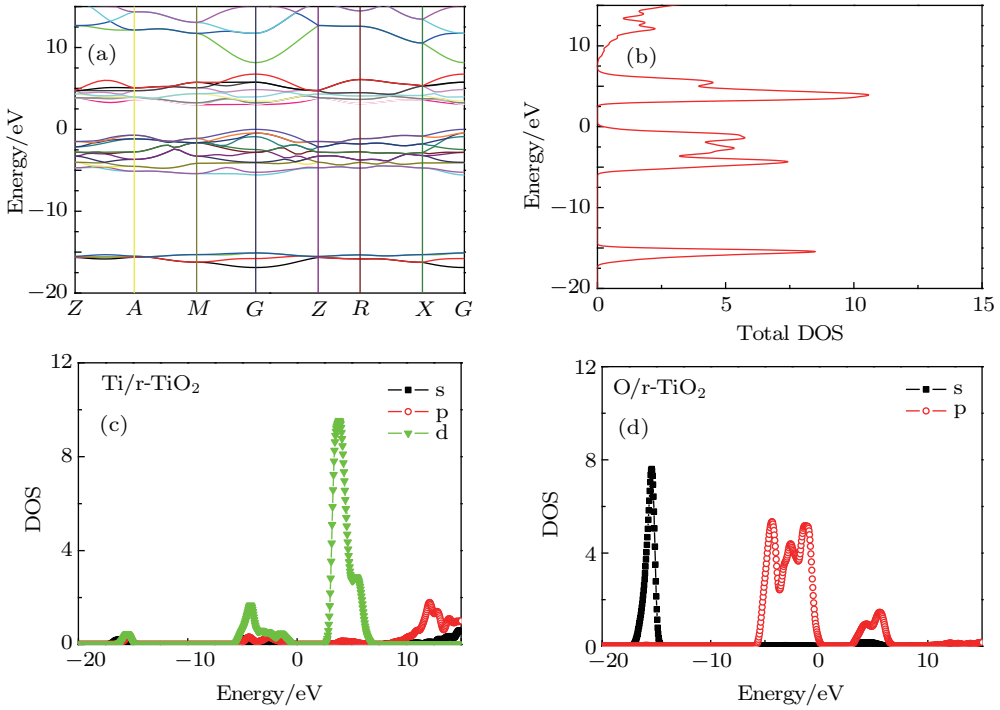


Fig. 2. (color online) The band structure and DOS of r-TiO_2 obtained by GGA+$U^d + U^p$ ($U^d = 6.75$ eV, $U^p = 3.5$ eV). (a) Band structure. The total DOS, the partial DOSs of Ti and O atoms are shown in panels (b), (c), and (d), respectively.

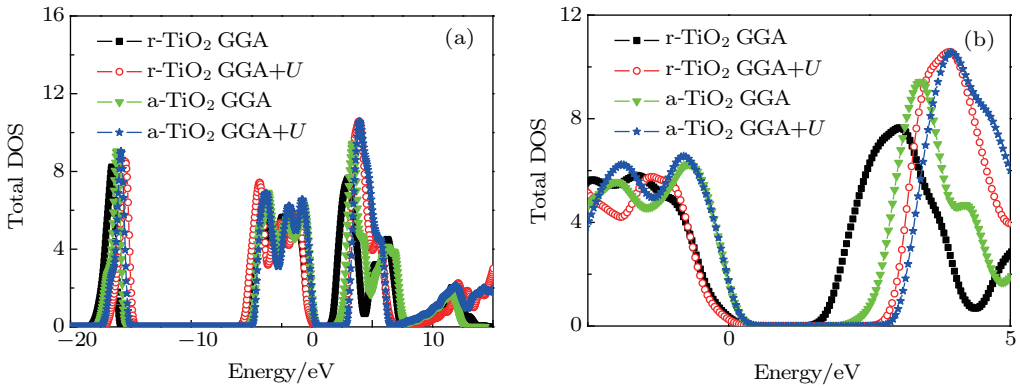


Fig. 3. (color online) Total DOSs of the two phases of TiO_2 by GGA without U, and GGA+$U^d + U^p$ ($U^d = 6.75$ eV, $U^p = 3.5$ eV, and $U^d = 7.75$ eV and $U^p = 1.0$ eV for r-TiO_2 and a-TiO_2, respectively) in a wide region (a), and zoom of the region near Fermi surface (b).

Figure 3 shows the comparison of the total DOSs between a- and r-TiO_2 obtained by GGA and GGA+$U^d + U^p$ ($U^d = 6.75$ eV, $U^p = 3.5$ eV, and $U^d = 7.75$ eV, $U^p = 1.0$ eV for r-TiO_2 and a-TiO_2, respectively). From the wide region (shown in Fig. 3(a)), the total DOSs of r-TiO_2 and a-TiO_2 obtained by GGA and GGA+$U^d + U^p$ look quite similar; while zooming into the region around the Fermi surface (Fig. 3(b)), we can see that compared with the results of GGA without U,

a significant change after including U is that the conduction bands are pushed to higher energies, which accordingly produces larger band gaps.

Figure 4 shows the dielectric function of r-TiO_2 obtained by GGA $+U^{\rm d}+U^{\rm p}$ ($U^{\rm d}=6.75$ eV and $U^{\rm p}=3.5$ eV) (a) parallel and (b) perpendicular components. The parallel and perpendicular components of the real part ε_1 have maximums of 12.53 at 3.86 eV and 10.98 at 3.94 eV, respectively. The calculated static dielectric constants are 6.298 and 5.485 along the different directions, coinciding with the experimental value 6.33.[24] The parallel and perpendicular components of the imaginary part ε_2 show the maximums of 10.28 at 6.74 eV and 9.50 at 4.90 eV, respectively. Other optical properties can be computed from the complex dielectric function.[25] For example, we can obtain the refractive coefficient of r-TiO_2, whose parallel and perpendicular components are $n_{\rm e}=2.75$ and $n_{\rm o}=2.46$. It is obvious that the values by GGA+$U^{\rm d}+U^{\rm p}$ are closer to the experimental values $n_{\rm e}=2.7$ and $n_{\rm o}=2.4$,[7] or $n_{\rm e}=2.76$ and $n_{\rm o}=2.44$.[26]

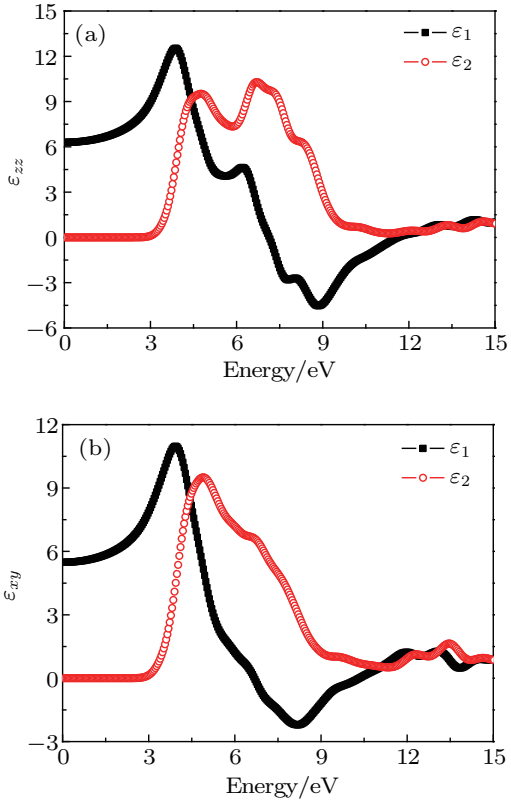


Fig. 4. (color online) Dielectric function of r-TiO_2 obtained by GGA+$U^{\rm d}+U^{\rm p}$ ($U^{\rm d}=6.75$ eV and $U^{\rm p}=3.5$ eV). (a) The parallel and (b) the perpendicular components.

Figure 5 shows the dielectric function of the parallel and perpendicular component in a-TiO_2 obtained by GGA $+U^{\rm d}+U^{\rm p}$ ($U^{\rm d}=7.5$ eV and $U^{\rm p}=1.0$ eV). From Fig. 5, we can see that the maximums of the parallel and perpendicular components of the real part ε_1 are 11.79 at 3.75 eV and 12.56 at 3.75 eV, respectively. The static dielectric constants of the two components are 6.137 and 5.995, coinciding with the experimental value 5.62.[24] The maximums of the parallel and perpendicular components of the imaginary part ε_2 are 10.29 at 4.74 eV and 11.22 at 4.52 eV, respectively. Other optical properties can be computed from the complex dielectric function.[25] The parallel and perpendicular components of the refractive coefficient of r-TiO_2 are $n_{\rm e}=2.34$ and $n_{\rm o}=2.29$. It is obvious that the values by GGA $+U^{\rm d}+U^{\rm p}$ are closer to the experimental values of $n_{\rm e}=2.32$ and $n_{\rm o}=2.28$.[27]

From Fig. 4 and Fig. 5, we can notice the optical anisotropies in both a- and r-TiO_2 between parallel and perpendicular components. The rutile form of TiO_2 has comparatively high anisotropy, both above and below the band gap, which makes r-TiO_2 a very useful optical material.[9] Below the band gap, r-TiO_2 has a large birefringence (difference between refractive indices of the parallel and perpendicular components) $\Delta n=n_{\rm e}-n_{\rm o}=0.29$ in our calculation, which is in good agreement with the experiment data ($\Delta n=0.27$[28] or 0.30[7]).

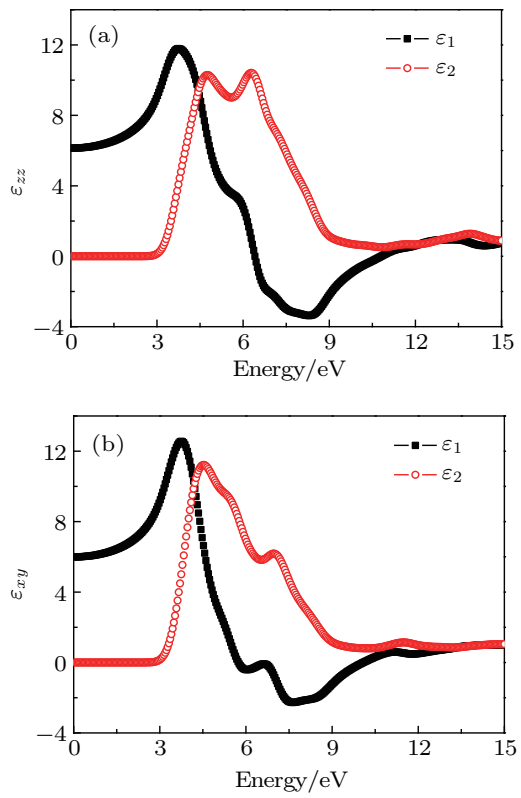


Fig. 5. (color online) Dielectric function of a-TiO_2 obtained by GGA+$U^{\rm d}+U^{\rm p}$ ($U^{\rm d}=7.5$ eV and $U^{\rm p}=1.0$ eV). (a) The parallel and (b) the perpendicular components.

To study the adaptability of the GGA+U approach, we further calculate the electronic structure of a titanium-vacancy and of hafnium-substitution solid solutions in rutile TiO_2. For titanium-vacancy solid solutions of rutile TiO_2, we first set 2×2×2 supercell. Namely, in one super cell, there are 16 titanium and 32 oxygen atoms. We delete only one Ti atom in the

center of the super cell, whose vacancy rate is 6.25%, and we obtain the electronic structure of titanium-vacancy solid solutions of rutile TiO_2 by GGA or by GGA+U ($U^{3d} = 7.0$ eV and $U^{2p} = 3.5$ eV for Ti 3d and O 2p, respectively) after geometry optimization. The calculation results are shown in Fig. 6(a).

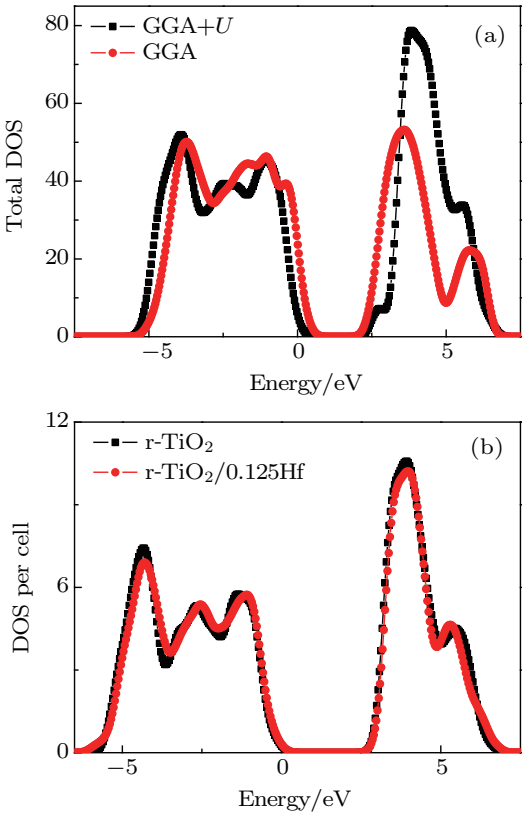


Fig. 6. (color online) (a) The DOS of r-TiO_2 with 6.25% vacancy by GGA and GGA+U; (b) the DOS of the pure r-TiO_2 and r-TiO_2 with 12.5% Hf doped by GGA+U.

The band gap of vacancy solid solutions by GGA and by GGA+U is 1.695 eV and 2.593 eV, respectively. As everyone knows, DFT (either by GGA or by LDA) usually undervalues the band gap. From Fig. 6(a), there are two clear sharps by GGA (in red color). If the GGA+U is used, the two sharps will merge together and the sharp height becomes bigger than those by GGA, much similar to our other works like cubic HfO_2[19] and monoclinic HfO_2.[29] For hafnium-substitution solid solutions in rutile TiO_2, we first set 2×2×1 super cell. Namely, in one super cell, there are 8 titanium and 16 oxygen atoms. We substitute only one Ti atom by hafnium in the center of the super cell, whose substitution rate is 12.5%, and we obtain the electronic structure of hafnium-substitution solid solutions and rutile TiO_2 by GGA+U ($U^{5d} = 8.0$ eV, $U^{3d} = 7.0$ eV, and $U^{2p} = 3.5$ eV for Hf 5d, Ti 3d, and O 2p, respectively) after geometry optimization. The calculation results are shown in Fig. 6(b). The band gap of the pure and Hf-doped rutile TiO_2 by GGA+U is 3.0 eV and 2.895 eV, respectively. From Fig. 6(b), we can see that the two lines are much similar between the pure and Hf-doped rutile TiO_2 by GGA +U. Considering the similar electronic configuration of Ti and Hf in the fourth subgroup with 4 valence electrons, it is reasonable that the pure r-TiO_2 has a very similar DOS with the doped one by 12.5% Hf. Besides, the calculated results of Mulliken atomic population in r-TiO_2 and the doped r-TiO_2 by 12.5% Hf are much similar, and the transfer charge of the O atoms in r-TiO_2 and the doped one by 12.5% Hf is −0.645 and −0.657, respectively.

4. Conclusion

The electronic structures and optical properties of anatase and rutile TiO_2 are calculated by means of first-principles generalized gradient approximation GGA and GGA) +U approaches. By GGA, the resulting band gaps E_g in a-TiO_2 and r-TiO_2 are around 2.16 eV and 1.85 eV, smaller than the experimental values. Introducing the Coulomb interactions of 3d orbitals on the Ti atom (U^d) and of 2p orbitals on the O atom (U^p), we can reproduce the experimental values of the band gap for a- and r-TiO_2. The best values for U^d and U^p are $U^d = 6.75$ eV and $U^p = 3.5$ eV, $U^d = 7.5$ eV and $U^p = 1.0$ eV for r- and a-TiO_2, respectively. The complex dielectric functions and refractive index of r-TiO_2 and a-TiO_2 are calculated. The results show optical anisotropy in both a-TiO_2 and r-TiO_2. The r-TiO_2 has relatively large anisotropy with birefringence $\Delta n = 0.29$, which makes it a useful optical material. We further calculate the electronic structure of the titanium-vacancy and of hafnium-substitution solid solutions in rutile TiO_2, and the calculation results show that the GGA+U approach has wide adaptability.

References

[1] Woan K, Pyrgiotakis G and Sigmund W 2009 *Adv. Mater.* **21** 2233
[2] Gumy D, Giraldo S A, Rengifo J and Pulgarin C 2008 *Appl. Catal. B: Environ.* **78** 19
[3] Meen T H, Water W, Chen W R, Chao S M, Ji L W and Huang C J 2009 *J. Phys. Chem. Solids* **70** 472
[4] Belcarz A, Bienias J, Surowska B and Ginalska G 2010 *Thin Solid Film* **519** 797
[5] Triyoso D H, Hegde R I, Zollner S, Ramon M E, Kalpat S, Gregory R, Wang X D, Jiang J, Raymond M, Rai R, Werho D, Roan D, White B E Jr and Tobin P J 2005 *J. Appl. Phys.* **98** 054104
[6] Cisneros-Morales M C and Aita C R 2008 *Appl. Phys. Lett.* **93** 021915
[7] Manuel Cardona and Gunther Harbeke 1965 *Phys. Rev. A* **137** 1467
[8] Noriko Hosaka, Takao Sekiya, Chikatoshi Satoko and Susumu Kurita 1997 *J. Phys. Soc. Jpn.* **66** 877
[9] Jellison G E Jr, Boatner L A, Budai J D, Jeong B S and Norton D P 2003 *J. Appl. Phys.* **93** 9537
[10] Chen H 2009 *Chin. J. Lumin. Sci.* **30** 697 (in Chinese)
[11] Zhang Y W, Yin C H, Zhao Q, Li F Q, Zhu S S and Liu H S 2012 *Acta Phys. Sin.* **61** 027801 (in Chinese)
[12] Keith M Glassford and James R Chelikowsky 1992 *Phys. Rev. B* **46** 1284
[13] Mo S D and Ching WY 1995 *Phys. Rev. B* **51** 13023
[14] Park S G, Blanka M K and Nishi Y 2010 *Phys. Rev. B* **82** 115109

[15] Song C L, Yang Z H, Su T, Wang K K, Wang J, Liu Y and Han G Ro 2014 *Chin. Phys. B* **23** 057101
[16] Xu Z C, Hou Q Y 2015 *Acta Phys. Sin.* **64** 157101 (in Chinese)
[17] Loschen C, Carrasco J, Neyman K M and Illas F 2007 *Phys. Rev. B* **75** 035115
[18] Segall M D, Lindan P J D, Probert M J, Pickard C J, Hasnip P J, Clark S J, Payne M C 2002 *J. Phys.: Condens. Matter* **14** 2717
[19] Li J P, Meng S H, Li L L, Lu H T and Tohyama T 2014 *Comput. Mater. Sci.* **81** 397
[20] Jeremy K Burdett, Timothy Hughbanks, Gordon J Miller, James W Richardson Jr and Joseph V Smith 1987 *J. Am. Chem. Soc.* **109** 3639
[21] Hyeok Choi, Elias Stathatos and Dionysios D Dionysiou 2006 *Appl. Catal. B: Environ.* **63** 60
[22] Tang H, Berger H and Schim P E 1993 *Solid State Commun.* **87** 847
[23] Diebold U 2003 *Surf. Sci. Rep.* **48** 53
[24] Wemple S H 1977 *J. Chem. Phys.* **67** 2151
[25] Wang J, Li H P and Stevens R 1992 *J. Mater. Sci.* **27** 5397
[26] Schubert M, Rheinlander B, Woollam J A, Johs B and Herzinger C M 1996 *J. Opt. Soc. Am. A* **13** 875
[27] Jellison G E, Boatner L A, Budai J D, Jeong B S and Norton D P 2003 *J. Appl. Phys.* **93** 9537
[28] Jellison G E Jr, Modine F A and Boatner L A 1997 *Opt. Lett.* **22** 1808
[29] Li J P, Han J C, Meng S H, Lu H T and Tohyama T 2013 *Appl. Phys. Lett.* **103** 071916